ELSEVIER

Contents lists available at ScienceDirect

Journal of Hydrology

journal homepage: www.elsevier.com/locate/jhydrol



Research papers



Spatio-temporal dynamics of hydrologic changes in the Himalayan river basins of Nepal using high-resolution hydrological-hydrodynamic modeling

Sanghoon Shin a,*, Yadu Pokhrel a,*, Rocky Talchabhadel b, Jeeban Panthi c

- ^a Department of Civil and Environmental Engineering, Michigan State University, East Lansing, MI, USA
- b Texas A&M AgriLife Research Center at El Paso, Texas A&M University, El Paso, TX, USA
- ^c Department of Geosciences, University of Rhode Island, Kingston, Rhode Island, USA

ARTICLE INFO

This manuscript was handled by Marco Borga, Editor-in-Chief, with the assistance of Massimiliano Zappa, Associate Editor

Keywords:
Himalayan hydrology
Nepal
Hydrological-hydrodynamic modeling
Flood dynamics
Terrestrial water storage
Groundwater depletion

ABSTRACT

The hydrology of the Himalayan region, known as the water tower of Asia, is undergoing rapid transformations due to climate change and growing human influences, and it is known that this region is one of those most vulnerable to climate change. Numerous studies have examined the changes in the hydrology of Nepal, which includes a significant upstream portion of the Himalayas. However, there is a lack of holistic studies on the spatial-temporal evolution of hydrologic dynamics over the entire nation and over long periods. In this study, we present a comprehensive assessment of the changes in river discharge, flood occurrence, and terrestrial water storage (TWS) across all river basins in Nepal using hydrological-hydrodynamic simulations spanning for 40 years (1979-2018) at \sim 5 km spatial resolution, and downscaled flood attributes at \sim 90 m resolution. The spatio-temporal variations in river discharge and inundation extent are examined through mapping of decadal trends using a quantile analysis method. The results indicate that the dynamics of river discharge has evolved varyingly across different river basins. The evolution pattern within a basin generally agrees with that at the basin outlet, but notable exceptions are found, indicating high hydro-climatic heterogeneity within the basins. The decadal evaluation of flood dynamics over major flooded areas suggests that inundation dynamics is strongly influenced by various flow characteristics, including the timing, duration, and magnitude, and that the evolution of flood dynamics is more complex than that of river discharge. Results indicate that the TWS dynamics over entire Nepal is strongly modulated by the variations in subsurface water storage, and groundwater storage has been in continuous decline (-1.74 cm/year) in the recent decades (2002-2016). This study provides a basis to advance the understanding of long-term hydrologic changes in the Himalayan region with important implications for improved water resources management.

1. Introduction

The Himalayan region, referred to as the water tower of Asia, supplies plentiful water to sustain river and groundwater systems in its downstream that provide water for human livelihood and critical ecosystems (Immerzeel et al., 2010; Viviroli et al., 2007). As the changes in the Earth's environment continue to alter the monsoonal rainfall patterns that strongly modulate the hydrology of the region (Ghosh et al., 2016, 2012; Mitra et al., 2012), the spatio-temporal dynamics of downstream water availability has become a topic of increasing concern (Dahal et al., 2018; Dimri et al., 2018a, 2018b; Immerzeel et al., 2014; Jeelani et al., 2012; Shrestha et al., 2012). Mounting evidence suggests that the Himalayan region is highly vulnerable to climate change (Roy

et al., 2019; Tewari et al., 2017). Among Himalayan countries, Nepal accounts for significant upstream portions of Himalayan region that has drastic elevation variation resulting in diverse climate (Karki et al., 2016) and land cover characteristics and biodiversity across the nation (Bonekamp et al., 2018; Immerzeel et al., 2015; Singh et al., 2019). Hence, understanding the hydrologic dynamics of river basins in Nepal is of utmost importance to provide a better understanding of the spatiotemporal changes in the Himalayan hydrology.

Surface water dynamics in Nepal is governed primarily by Himalayan snowmelt and monsoon rainfall. The four major river basins, namely the Mahakali, Karnali, Gandaki, and Koshi (Fig. 1), originate in the upper Himalayan region receiving substantial snow and glacier melt water, flow through rugged terrains in the central hilly areas of Nepal,

E-mail addresses: shinsa11@msu.edu (S. Shin), ypokhrel@egr.msu.edu (Y. Pokhrel).

^{*} Corresponding authors.

and drain into the Ganges river system in India. Overall, the hydrologic dynamics of these river systems is strongly modulated by the rhythm of the South Asian monsoon that brings $\sim 80\%$ of the annual rainfall during the monsoon season (June-September) (Panthi et al., 2015; Shrestha, 2000). The intense monsoonal rains produce a typical unimodal hydrograph with a sharp rise in flow volumes, often causing widespread flooding (Dhital and Kayastha, 2013). During the dry season, flows reduce appreciably, affecting downstream agricultural systems and causing issues for sustaining hydropower generation (Dahal et al., 2020; Poudyal et al., 2019).

The large climate and topographic gradient, young geological formations, and strong monsoon effect make the river basins of Nepal highly susceptible not only to adverse climatic impacts (e.g., floods, droughts) but also to natural hazards including glacial lake outburst flood (GLOF) and excessive soil erosion (Agarwal et al., 2016; Chen et al., 2013). As the nation is undergoing rapid socio-economic growth, the threats of climate change impacts are further exacerbated by humaninduced changes in land-water systems due to expanding agriculture, urbanization, and construction of dams for hydropower generation and irrigation, which are all inevitable to support the growing needs for food, water, and energy (Chinnasamy et al., 2015; Dhakal et al., 2019; Paudel et al., 2016). Moreover, the transboundary nature of the Mahakali, Karnali, Gandaki, and Koshi basins—that share some portions with China and India-adds further challenges in making optimum use of resources among different regions while also considering the ecosystem needs. As such, these ongoing climate shifts and human-induced alterations of land-water systems have altogether resulted in an increasing threat to the region in terms of water and food security and ecological

Analysis of long-term observational data provides an insight for historical evolution; however, hydrometeorological observations are generally scarce in terms of both spatial and temporal coverages, especially for regions like Nepal. In this vein, hydrological models are indispensable tools for understanding the long-term evolution of such complex and large-scale hydrologic systems. Indeed, large-scale hydrologic studies have benefited from the advances made in hydrological modeling over the past two decades (Nazemi and Wheater, 2015; Pokhrel et al., 2017, 2016; Wada et al., 2017). In case of the Himalayan region, and specifically for Nepal, most studies have relied on limited observations (e.g., Karki et al., 2020; Sharma and Shakya, 2006), and modeling studies have not fully exploited the advances in recent model developments. The outstanding challenges and limitations of existing

hydrologic and hydrodynamic studies in Nepal are primarily related to: (1) a focus on river flow as the sole variable to describe the changing hydrology in the region (e.g., Bajracharya et al., 2018; Palazzoli et al., 2015; Pandey et al., 2019; Rajbhandari et al., 2017; Sharma and Shakya, 2006; Shrestha et al., 2016a, 2016b, 2014, 2013), and (2) sub-national scale studies focusing on a part of the country (e.g., Babel et al., 2014; Bharati et al., 2016; Bhatta et al., 2019; Chinnasamy et al., 2015; Mishra et al., 2018).

Regarding to the first issue identified above, among many observation- and modeling-based studies in Nepal, most have focused on changes in river flow. While river flow is a key indicator of water availability, there are other hydrologic variables such as surface water depth, inundated area, and river-floodplain water storage that provide a more comprehensive representation of the spatial and temporal changes in water resource systems. For example, Pandey et al. (2011) assess the adaptive capacity of water resources system of the Bagmati river basin, by using area of vegetation and wetland as a proxy for ecological capacity due to the limitation of data availability. With the high-resolution modeling, variables such as the natural water availability can be explicitly derived from the simulated spatio-temporal distribution of water storages, which are useful for water resources management and ecological applications (Bharati et al., 2014). As for the second issue, hydrological simulations have generally been conducted for a portion of the nation. To cope with the aforementioned compounded pressures, it is essential to develop a holistic understanding of the long-term and nationwide hydrologic changes since many water-related problems are multi-sectoral that should be addressed at the local, national, and regional scales (Friedman et al., 1984; Henriksen et al., 2003; McMillan et al., 2016). The increased domain size also provides an opportunity to utilize the terrestrial water storage (TWS) measurements from the Gravity Recovery and Climate Experiment (GRACE) satellites, rarely used by previous studies in Nepal. As such, the simulation of the hydrologic systems across all basins can provide a holistic view at the national level.

The objective of this study is to present a comprehensive analysis of the spatio-temporal changes in hydrologic fluxes and storages across all river basins of Nepal and for a multi-decadal historical period. The results are based on high-resolution integrated hydrological-hydrodynamic modeling validated against ground- and satellite-based observations. Key research questions addressed in this study are follows. (1) How has the dynamics of natural river discharge, inundated areas, and TWS in the Himalayan river basins of Nepal evolved over the

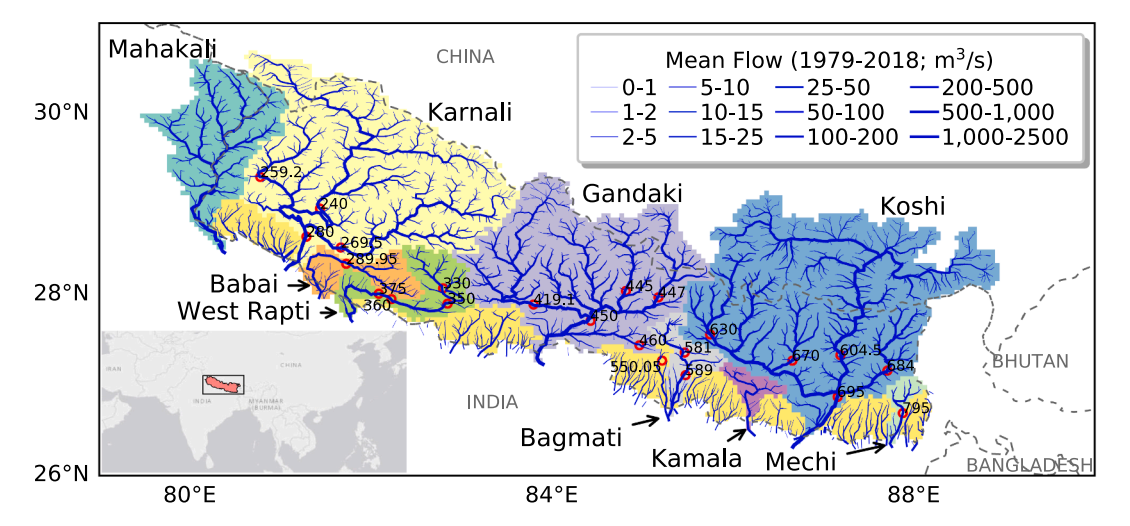


Fig. 1. The river basins of Nepal. Location of the basins is indicated in the lower left conner. The background color coding indicates the spatial extent of the basins. Blue lines with varying widths show the spatial distribution of long-term mean (1979–2018) river discharge at ~ 5 km grids. Red circles mark the location of hydrological gauging stations; the numbers indicate the station IDs used in the database of the Department of Hydrology and Meteorology (DHM), Nepal. (For interpretation of the references to color in this figure legend, the reader is referred to the web version of this article.)

past four decades? (2) Are there any distinct spatial patterns and temporal signatures in low, median, and high river flows in those river basins? (3) What are the similarities in inter-annual and decadal trends across the river basins located in different geographic regions? We answer these questions based on the simulation results of the historical river-floodplain dynamics for 40 years (i.e., 1979–2018 period) at a spatial resolution of $\sim 5~{\rm km}$ (3 arc-minute), where flood extent is downscaled to a further finer resolution of $\sim 90~{\rm m}$ (3 arc-second). Such advanced capability of high-resolution hydrological modeling for a large domain is enabled by combining a global land surface model HiGW-MAT (Pokhrel et al., 2015) and a global river-floodplain hydrodynamic model CaMa-Flood (Yamazaki et al., 2011).

To our best knowledge, this is the first study of such kind to use highresolution simulations of river-floodplain dynamics over the entire Nepal, in which not only the changes in river discharge but also inundated areas and river-floodplain water storages are examined. Through the high-resolution modeling over the nationwide domain, we provide important advances over previous studies in the region in that the simulations are conducted in a consistent modeling framework, which allows collective comparisons of basin-wise characteristics of hydrological responses. This enables the understanding of how the hydrology in the region has evolved historically, which is a key to future projections of water resources and hence sustainable development and climate change adaptation. In the remainder of this paper, the models (HiGW-MAT and CaMa-Flood) are introduced, and observational data and research approach are described in section 2. Results and discussions are provided in section 3, and summary and conclusion are presented in section 4.

2. Materials and methods

2.1. HiGW-MAT and CaMa-Flood models

HiGW-MAT (Pokhrel et al., 2015) is a global land surface model that simulates various hydrological processes from canopy to bedrock on a full physical basis by solving both energy and water balances. CaMa-Flood (Yamazaki et al., 2013, 2011) is a global hydrodynamic model, which computes river-floodplain hydrodynamics (i.e., river discharge, flow velocity, water level, and inundated area) by solving shallow water equations of open channel flow, explicitly accounting for backwater effects using the local inertial approximation (Yamazaki et al., 2013). We use a modeling framework that combines HiGW-MAT and CaMa-Flood. Such integration provides an optimal combination in terms of spatial resolution needed to resolve key hydrological processes at different scales. HiGW-MAT is used to simulate local runoff by considering hydrological processes such as evapotranspiration, snow melt, infiltration, and groundwater dynamics at a resolution of 0.5° (~50 km) that is consistent with that of meteorological forcing, namely the WATCH Forcing Data using the ERA-Interim (WFDEI) data (Weedon et al., 2018). The runoff from HiGW-MAT is then used in CaMa-Flood to simulate the finer details of river-floodplain processes at a high resolution of 3-arcmin (~5km) because the focus of the present study is river discharge and floodplain processes. This model combination has been widely used for regional to global-scale studies (Burbano et al., 2020; Pokhrel et al., 2018; Shin et al., 2020; Yamazaki et al., 2014, 2012; Zhao et al., 2017). Such multi-scale modeling approach allows the simulations of long-term changes in terrestrial water storage and flux at high resolution over the large domain with less computational burden.

HiGW-MAT derives from MATSIRO (Minimal Advanced Treatments of Surface Interaction and Runoff; Takata et al., 2003), which has been advanced over the years by adding various new schemes to simulate groundwater flow and human water management. Each grid cell of HiGW-MAT has four types of surfaces with and without canopy and snow, respectively, where energy fluxes are calculated separately considering sub-grid heterogeneities. Canopy interception and transpiration are estimated based on the photosynthesis scheme in the Simple

Biosphere Model 2 (SiB2; Sellers, 1997), surface and subsurface runoff processes are modeled using a simplified TOPMODEL (Beven and Kirkby, 1979; Stieglitz et al., 1997), soil moisture movement is simulated by solving the Richards equation (Koirala et al., 2014; Richards, 1931; Yeh and Eltahir, 2005), and the water table depth is explicitly represented (Koirala et al., 2014). HiGW-MAT includes the capability to simulate human water management practices (Pokhrel et al., 2012a, 2012b, 2015), but we use HiGW-MAT in the natural setting (i.e., the human water managements modules are turned off) following our previous studies to provide runoff forcing to CaMa-Flood (Pokhrel et al., 2018; Shin et al., 2020) since our objective is on investigating the hydrological changes stemming from natural climate variability, which is the first order driver of flow regime change (Bower et al., 2004). Landsurface properties, including land cover, soil type and associated model parameters, are set to identical to those in our previous studies (Pokhrel et al., 2018; Shin et al., 2020).

We use CaMa-Flood version-3.94 with a spatial resolution of ~ 5 km, which includes the capability to downscale flood depth to a further higher resolution of 3-arcsec (~90 m). For river-floodplain parameterizations (e.g., flow direction, river-floodplain elevation profile, river length, and river width), MERIT Hydro is used, which is a global hydrography dataset based on the MERIT (Multi-Error-Removed Improved-Terrain; Yamazaki et al., 2017) DEM (Digital Elevation Model) and multiple inland water body datasets (Yamazaki et al., 2019). As errors including absolute bias, stripe noise, speckle noise, and tree height bias (Yamazaki et al., 2017) that prevail in the previously used SRTM (Shuttle Radar Topography Mission) DEM are removed, an improved simulation of river-floodplain dynamics is enabled. A complete description of the model physics, parameterization methods, and sensitivities to input parameters in CaMa-Flood can be found in the previous literature (Yamazaki et al., 2013, 2011) and the user manual that is available for free download.

2.2. Observational data

Simulated river discharge is validated against the observational data at 23 gauging stations maintained by the Department of Hydrology and Meteorology (DHM), Nepal (Fig. 1). The gauging stations are evenly distributed in both upstream and downstream regions, and they include at least 16 years of data records.

The Global Surface Water (GSW) data (Pekel et al., 2016) are used to validate the simulated flood extent at ~ 90 m resolution. The GSW data are based on Landsat satellite images from 1984 to present for the entire globe. Each pixel of Landsat images is classified either as open water, not open water, or non-valid class. For valid classes (i.e., open water and not open water), classification results are combined on a monthly basis as a form of frequency of open water existence at a pixel. Here, we calculate the flood occurrence from the modeled flood extents and compare it with the flood occurrence of GSW data for the identical period, i.e., 1984-2018. Due to the difference in spatial resolutions of the GSW data (0.0025°) and CaMa-Flood $(0.00083^\circ$ or 3-arcsec), the GSW data are upscaled to 0.0010° for the convenience of comparison.

Simulated TWS anomaly is compared with the data inferred from the GRACE satellite mission. We use the mascon products, which have advantages over traditional spherical harmonics products (Jing et al., 2019; Scanlon et al., 2016), and are available from two different processing centers, the Jet Propulsion Laboratory (JPL) and the center for Space Research (CSR) (Save et al., 2016; Watkins et al., 2015). As the use of multiple GRACE products is recommended for a basin-scale application (Scanlon et al., 2016), TWS anomaly is derived from the mean of the two mascon products using area-weighted average over the modeling domain (Chaudhari et al., 2019). For comparison with GRACE, the simulated TWS is first calculated by summing up canopy water, snow water, and subsurface water storages from HiGW-MAT and riverfloodplain storage from CaMa-Flood, following Pokhrel et al. (2018). Then, the simulated TWS anomaly is calculated as the deviation from

mean of the simulated TWS during 2004-2009.

2.3. Estimation of groundwater storage variations

While the TWS from GRACE provide the total TWS as vertically-integrated values of all relevant TWS components (i.e., canopy, snow, soil, river-floodplain, and ground water storages), the simulated results include explicitly resolved individual storage components. Hence, the simulated results provide additional insights on the component contribution of different water storages to the total TWS. However, the effects of water management activities, specifically groundwater withdrawal, which are captured in the GRACE data are not simulated in the models (see Section 2.1). Thus, we estimate the variations in groundwater storage caused by both natural variability and groundwater withdrawal following Rodell et al. (2009). In this approach, groundwater storage variations are isolated by subtracting the other water storage components from model simulations (i.e., canopy, snow, soil, and riverfloodplain water storages) from GRACE TWS.

2.4. Statistical analysis methods

2.4.1. Quantile analysis of river discharge

To understand and visualize the historical evolution of river discharges at the major basin outlets, we adopt and modify a quantile analysis method by Rottler et al. (2019), which combines quantile sampling, trend analysis, and Complete Ensemble Empirical Mode Decomposition with Additive Noise (CEEMDAN) (Colominas et al., 2014; Torres et al., 2011). The method enables analysis and visualization of the (1) long-term seasonality, (2) trend of seasonality change, (3) temporal evolution of seasonality, and (4) annual flow duration curve. To do so, three different quantiles are defined, which vary from 0.01 (small discharge) to 0.99 (large discharge): quantile on a daily basis (QDAY), quantile within 30-day moving window (QMOV), and quantile on a yearly basis (QYEA).

The long-term seasonality of river discharge in different basins is directly illustrated by representing QDAY with respect to DOY (day of year). QDAY is calculated for each DOY without differentiating the years, e.g., QDAY for May 16th is calculated from 40 values for May 16th of each year during the 1979–2018 period. By using QDAY, the seasonality at different level of quantiles can be represented at once.

The trend of seasonality change is assessed from a trend analysis of QMOV. QMOV is calculated for each DOY and each year, e.g., QMOV for May 16th, 2001 is calculated among the values during its \pm 15 days (i.e., from May 1st, 2001 to May 31st, 2001); QMOVs for May 16th of the other years other than 2001 are independently calculated. For the trend analysis, the Theil-Sen method (Sen, 1968) is used, which is less sensitive to outliers than the least square method. By compiling the results from different DOYs and probabilities, the long-term trend of seasonality change can be represented with respect to different quantile levels.

To supplement the trend analysis, the temporal evolution of seasonality is investigated for 30-day moving average time series. From the average daily time series, the yearly time series for each DOY is extracted, e.g., the 30-day averaged river discharge for May 16th of each year. Here, we use the CEEMDAN method to investigate the temporal evolution of seasonality. We note that CEEMDAN decomposes the time series into a collection of intrinsic mode functions (IMFs), and the last IMF, which is also referred to as the residue, represents the trend of data; the increasing residue values compared to the values in their prior years indicate an increasing trend, and vice versa. The residue of CEEMDAN can be nonmonotonic (e.g., U-shaped curve), increase/decrease abruptly at a certain year, and flat. Hence, the temporal evolution of seasonality can be assessed at diverse aspects. When the residues of CEEMDAN for different DOYs are compiled together, the deviation of residue of CEEMDAN for 30-day averaged flow (hereafter δ_{30d}) is presented for comparisons. To test the existence of monotonic trend, the Mann-Kendall (MK) test is used ($\alpha = 0.05$).

The change of annual flow duration curve is investigated using QYEA. QYEA is essentially identical to an empirical flow duration curve, derived from daily data for a year. QYEA is calculated for each year without differentiating DOY, e.g., QYEA for 2001 is calculated among 365 values in the year; QYEAs for the other years are independently calculated. The yearly time series of QYEA is analyzed using CEEMDAN method for each quantile, and the deviation of residue of CEEMDAN for QYEA (hereafter δ_{1yr}) from every quantile is compiled and presented. The MK test is used to assess the existence of monotonic trend.

Note that the plots are provided in two forms: original values as in Rottler et al., (2019) and standardized values. The standardization is conducted to make dry-season flows and small-quantile flows more discernible when they are plotted together with wet season flows and high quantile flows. For standardization for the trend of seasonality change and the temporal evolution of seasonality, a given value is divided by the mean of the values having the identical DOY. For the change of annual flow duration curve, a given value is divided by the mean of the values having the identical exceedance probability.

2.4.2. Mapping of Multi-Decadal change

To examine the overall spatio-temporal dynamics of river discharge across the nation, we map the multi-decadal trends in low $(Q_{10}; 10\%)$ quantile in QYEA), median (Q50; 50% quantile) and high (Q90; 90% quantile) flows at all ~ 5 km grid cells for every decade (10-year periods during 1979-1988, 1989-1998, 1999-2008, and 2009-2018). The decadal trend maps are generated from the trends in δ_{1vr} (Section 2.4.1), estimated by using the Theil-Sen method. The existence of monotonic trend for each decade is examined using MK test ($\alpha = 0.05$). The use of trend maps for low, median, and high flows and for four different decadal periods enables an explicit representation of the overall evolution of river discharge at the \sim 5 km grids. Since the decadal trend is calculated as the rate of change within a given decade, four snapshots are obtained for each quantile. Similarly to that for the decadal trends in river discharge, we calculate the change in flood occurrence from one decade to the next that results in three snapshots of flood occurrence change between the decadal periods.

3. Results and discussion

3.1. River discharge

3.1.1. Validation of river discharge

Evaluation of river discharges at 23 gauging stations is presented in Fig. 2. The spatial distribution of long-term mean river discharge over the entire basins is presented in Fig. 1, also indicating the locations of the gauging stations. As high coefficients of determination indicate (R^2 > 0.9), the seasonal cycle of river discharge is well reproduced not only at relatively downstream locations but also at small tributaries. Specifically, the low flow is simulated remarkably well at most locations, which is important for water resources management such as irrigation and hydropower operation. Note that the models are not tuned using observations and applied over a relatively large domain, and the hydrologic processes are simulated by a land surface model using global forcing datasets. Hence, a perfect match with observations is not expected. Further, since the primary objective of this study is to examine the interannual variabilities in river discharges, certain discrepancies in the flow seasonality are not of particular concern. In quantifying the interannual variabilities, analyzing differences in river discharge among different years can offset consistent overestimation or underestimation tendencies. Hence, we consider the results to be of reasonable accuracy overall to investigate the long-term evolution of river discharge.

3.1.2. Evolution of river discharge over four decades

Fig. 3 shows the long-term seasonality, trend of seasonality, temporal evolution of seasonality, and change of annual discharge for the four major river basins. From the long-term seasonality, the wet season is

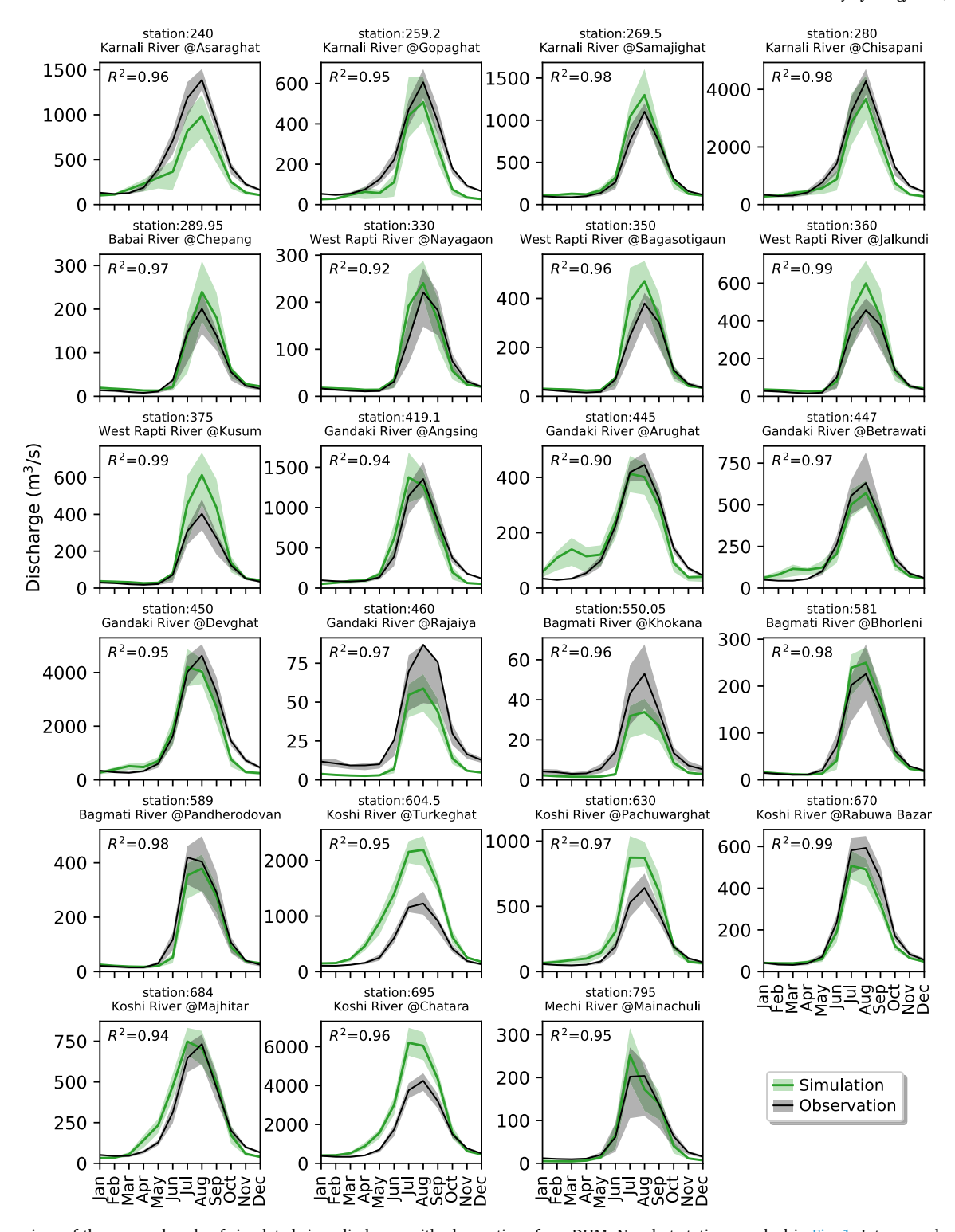


Fig. 2. Comparison of the seasonal cycle of simulated river discharge with observations from DHM, Nepal at stations marked in Fig. 1. Interannual variability is indicated by green and grey shadings for simulated and observed discharge, respectively, using upper and lower 25% flow quantiles for each month. Coefficient of determination (R²) is indicated for every station. (For interpretation of the references to color in this figure legend, the reader is referred to the web version of this article.)

evidently found to be June, July, August, and September (JJAS) across the nation (Fig. 3a). High quantile flows (i.e., high discharge) and the wet season flows (i.e., JJAS) are found to have decreased in all four basins (Fig. 3b). Overall QMOV trends are negative, except for some high quantile flows in the dry season (i.e., other than JJAS) where increasing trends become more noticeable as a basin is located farther east. The prevalent decreasing QMOV trends indicate the nationwide

decrease in seasonal river discharge. The increase in high quantile flows in the dry season suggests a tendency of increased flooding in the dry season with a higher magnitude in recent times than in the past.

The findings on river discharge evolution from QMOV trends are explained in a greater detail in terms of the evolution of δ_{30d} (Fig. 3c). It is worth recalling that the increasing values of δ_{30d} compared to the values in their prior years indicate an increasing trend, and vice versa.

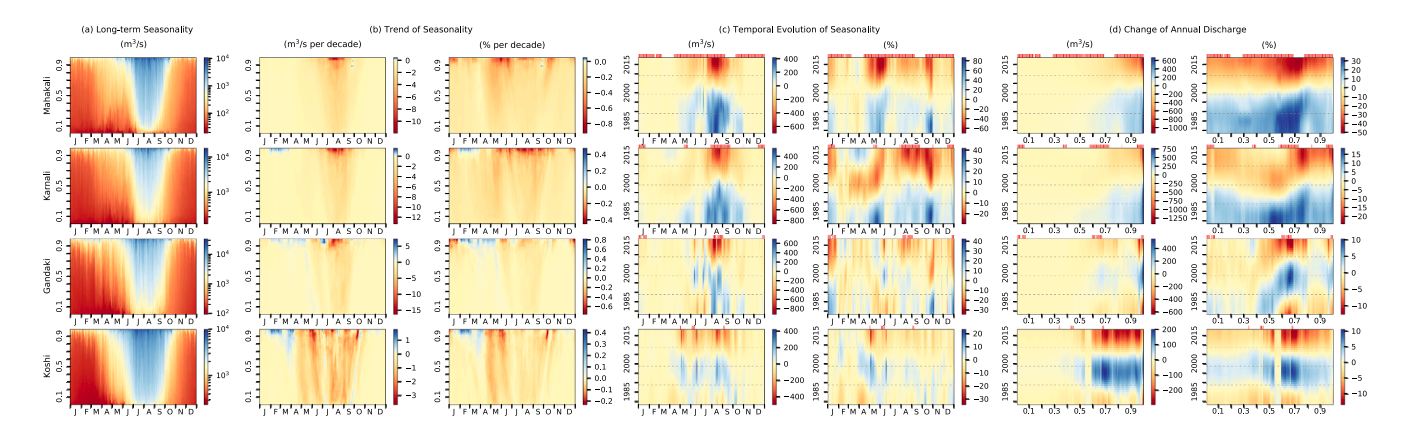


Fig. 3. Evolution of river discharge at the outlets of four major river basins in Nepal over the 1979–2018 period. (a) Long-term seasonality, (b) trend of seasonality, (c) temporal evolution of seasonality, and (d) change of annual discharge. The left and right panels in each subject present the values without and with standardization. Red and blue bars on top of the subplots in (c) and (d) indicate significant monotonic decrease and increase, respectively, over the 40 year period at a given DOY (day of year) (Mann-Kendall test; $\alpha = 0.05$). Gray dash lines in the subplots in (c) and (d) indicate decadal periods from 1979 to 2018. (For interpretation of the references to color in this figure legend, the reader is referred to the web version of this article.)

Interestingly, during the latest two decades (1999–2018), all basins show decreasing δ_{30d} in the wet season (Fig. 3c). Other than that, a basin further to the west tends to have a more consistent decreasing trend than that in the basins to the east (more red bars in Fig. 3c). In addition to geological location, as the time windows of interest moves towards the dry season, the transition patterns of δ_{30d} become rather mixed (e.g., decrease followed by increase in February-April at Karnali basin).

The change in annual flow duration curve is found to vary according to the basin locations (Fig. 3d). Note that increasing δ_{1yr} over time at a given quantile indicates an increase in QYEA, and vice versa. Overall, a considerable decrease in QYEA is found for the Mahakali basin at most of quantiles from mid-1990 s through mid-2010 s (Fig. 3d). Such transition over a decade is also found in the Karnali basin, but the timing varies according to the quantiles; some quantiles vary from early-1990 s and others vary from early-2000 s. The Karnali basin shows another distinct change pattern at the quantiles from 0.3 to 0.6 in 2010 s, where QYEA increases in recent years. The Gandaki basin shows mixed trends; decreasing trends are found at quantiles between 0.4 and 0.5 in the 1990 s, between 0.5 and 0.8 and greater than 0.95 in the 2000 s, and

between 0.8 and 0.95 in the 2010 s; increasing trends are also found at quantiles between 0.5 and 0.8 and greater than 0.9 that last until the early-1990 s. The Koshi basin shows similar trends in QYEA for all quantiles; increasing trends lasting until the mid-1990 s are followed by decreasing trends in the 2000 s. In sum, the annual flow duration curves of the major river basins of Nepal are found to have evolved varyingly in the past four decades.

Spatial distribution of decadal trends in low, median, and high flows are presented in Fig. 4. In general, the decadal trends within the basins are similar to those at the basin outlets, hence the overall observations from Fig. 3d apply also to these results. For example, it is evident that low, median, and high flows in the downstream regions have persistently declined during the last two decades (1999–2018), which is in line with what can be seen in Fig. 3d. Such nationwide decrease in river flow has an important implication for water resource management, especially for hydropower development and irrigation. Specifically, hydropower operation can be considerably limited by the decrease in low flow during the drying season due to the environmental flow requirement. It is, however, worth noting that the trends at the basin outlets do not

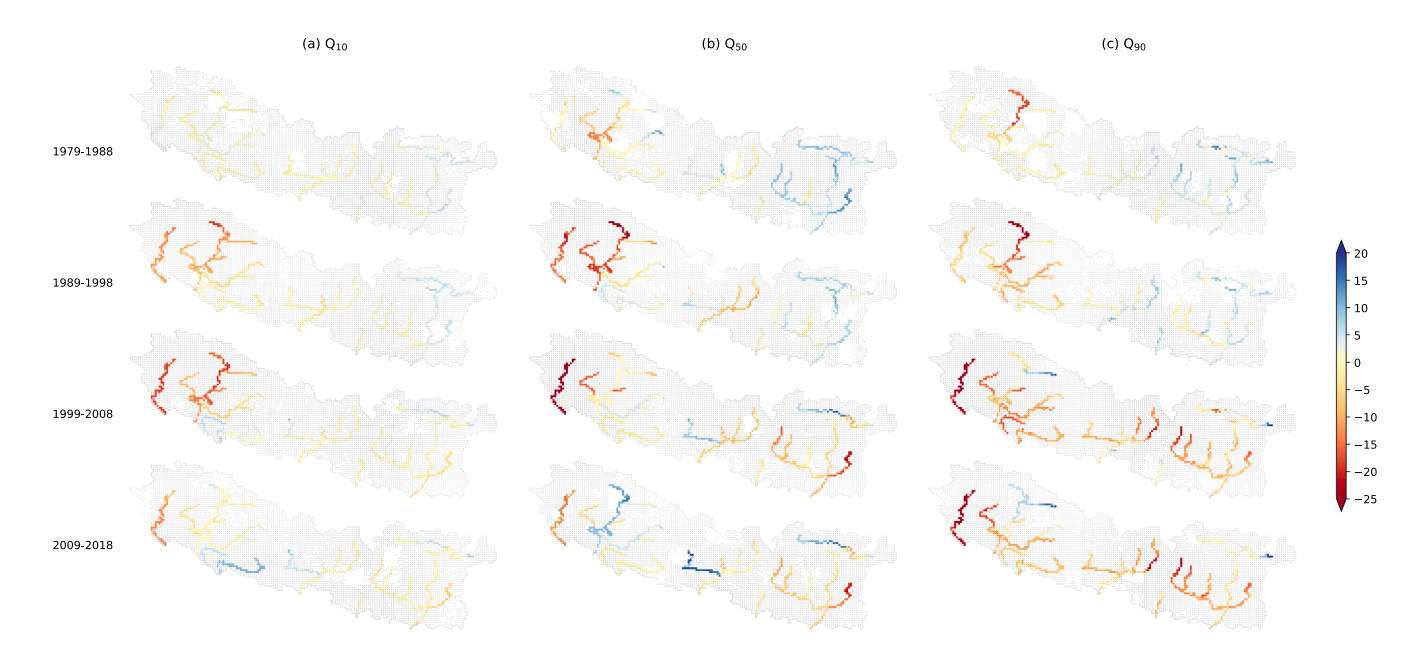


Fig. 4. Decadal trend in (a) low flow (Q_{10}) , (2) median flow (Q_{50}) , and (3) high flow (Q_{90}) calculated from the quantiles on a yearly basis (QYEA). Significant monotonic changes are indicated with black dots (Mann-Kendall test; $\alpha = 0.05$). The unit is percentage change per decade. Small river reaches with $Q_{10} < 10 \text{ m}^3/\text{s}$ are pruned out.

necessarily represent the trends over the entire basin. For example, the opposite trends at the basin outlets and a part of basins are found for northern part of Karnali, western part of Gandaki, and northern part of Koshi basins. Such prevalent opposite trends within the basins compared to those at the basin outlets suggest substantial hydrological heterogeneity across the nation.

3.2. Water storage dynamics

3.2.1. Inundated areas

Fig. 5 shows the first results of the long-term river-floodplain storage over all Nepalese river basins for the 1979-2018 period. For selected regions, the simulated flood occurrences from CaMa-Flood are compared with the GSW data for the 1984-2018 period (Fig. 6). The broad spatial patterns of natural river-floodplain storage are well captured by the model for large river basins. In the downstream portions of the basins—where floodplains are more developed than in the upper reaches—the maximum flood extent and seasonally inundated areas are relatively prominent (Fig. 5). Some differences are found between flood occurrences simulated by CaMa-Flood and GSW data. The differences can be attributed partly to the errors in DEMs used in CaMa-Flood, but the GSW product also suffers from limitations in the Landsat satellite images, which are susceptible to atmospheric conditions (i.e., cloud cover) and are known to have substantial missing records specifically until early 2000 s (Shin et al., 2020); the former generally results in the underestimation of GSW flood occurrence and maximum flood extent specifically for the wet season, and the latter is suggested to cause general biases in the GSW flood occurrence specifically towards the recent years. Large water bodies are reproduced by the model, but gradation of flood occurrence around the rim of those water bodies, seen in the GWS data, is underrepresented in the simulated results (e.g., west region in Fig. 6a; middle region in Fig. 6d). This is because of the hydrography data, i.e., MERIT DEM and MERIT Hydro. MERIT DEM is based on Shuttle Radar Topography Mission (SRTM) DEM, launched in 2000, and some other DEM products (Yamazaki et al., 2019, 2017). Thus, elevation variations over a region where large water bodies existed before year 2000 are indicated as flat areas such that water spreads over those regions in CaMa-Flood simulation.

For the selected regions, we further investigate how the inundation dynamics evolved over time. Fig. 7 presents the decadal changes in flood occurrence. Overall, the change in flood occurrence is found to have

resulted from the combined effects of river discharge changes at different quantiles. When high flow (e.g., Q_{90}) increases, the maximum inundation extent increases and the regions near the maximum extent are inundated more frequently, and hence the flood occurrence in those regions increases, and vice versa. Meanwhile, when the duration of low-to-median flows (e.g., Q_{10} - Q_{50}) increases, the regions near river channels are inundated for a longer time so that the flood occurrence increases, and vice versa. Overall, the diverse spatial patterns of the changes in flood occurrence reflect various aspects of hydro-climatic changes over the nation. Such investigation on the evolution of inundation dynamics over 40 years is enabled by the high-resolution simulation of river-floodplain processes.

3.2.2. Terrestrial water storage (TWS)

To understand how TWS-an integrated measure of overall water availability—is changing across all basins, we examine the TWS anomalies from the models (see Section 2.1) and those from GRACE satellites. Fig. 8 presents a comparison of simulated and GRACE-based TWS anomalies for 2002-2016 (a period chosen considering GRACE data availability) and averaged over all Nepalese river basins (Fig. 1). Model results suggest that subsurface water storage (i.e., soil moisture and ground water storage) strongly dominates the overall TWS dynamics. That is, compared to subsurface water storage, the variations in the other storage components (i.e., canopy, river-floodplain, and snow storages), are relatively small. The contribution of individual components to total TWS varies spatially depending on climate, topography, and level of human impacts. The component contributions in the Nepalese basins—a relatively higher contribution of sub-surface storage-are found to be similar to those in other basins located in comparable latitudes (Felfelani et al., 2017; Ferreira et al., 2020). In terms of within-a-year variability, the simulated results well capture the general seasonal variations in TWS seen in GRACE data; however, in terms of interannual variability, continually decreasing trends in the GRACE data are not found in the simulated results. This suggests that the decreasing trend in the GRACE TWS is likely caused by growing groundwater exploitation (Pandey et al., 2010; Prasad Pandey and Kazama, 2014; Shrestha et al., 2020), the effects of which are captured in GRACE data but not simulated in the model.

Model results indicate an increase in TWS (and groundwater) during the 2002–2016 period, with a trend of 0.18 (0.11) cm/year, which resulted from an initial decline at the rate of -0.21 (-0.10) cm/year

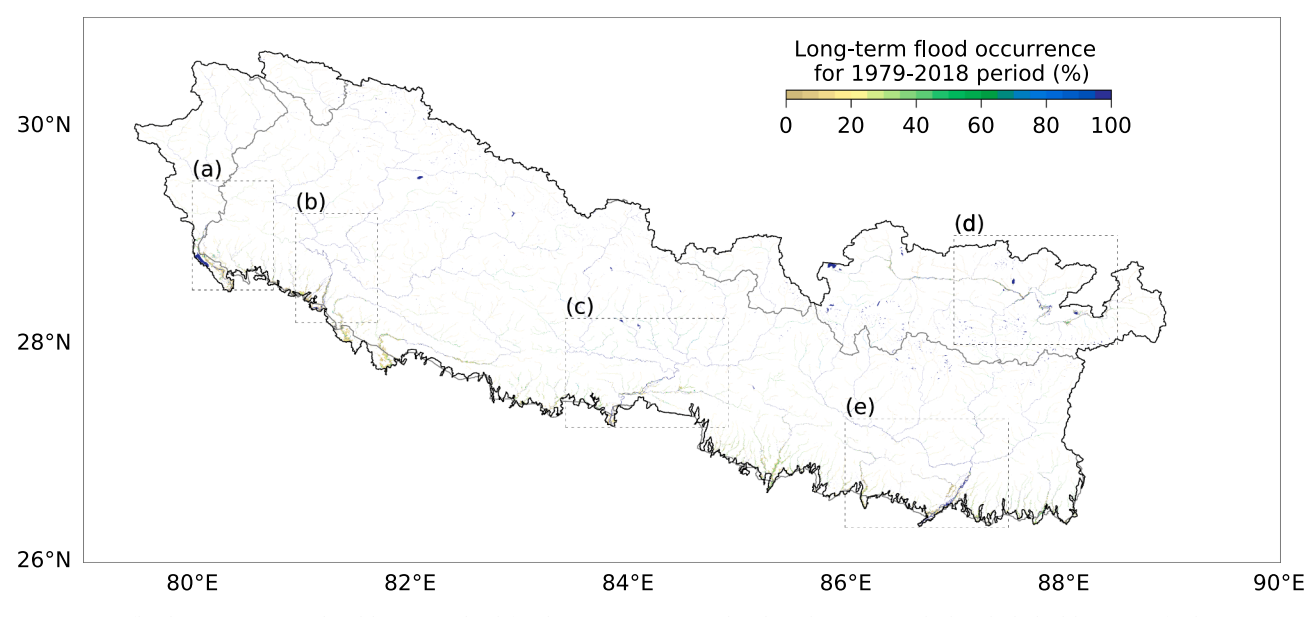


Fig. 5. Long-term flood occurrence simulated by CaMa-Flood for the 1979–2018 period. Selected regions marked with dashed boxes are further investigated in Figs. 6-7.

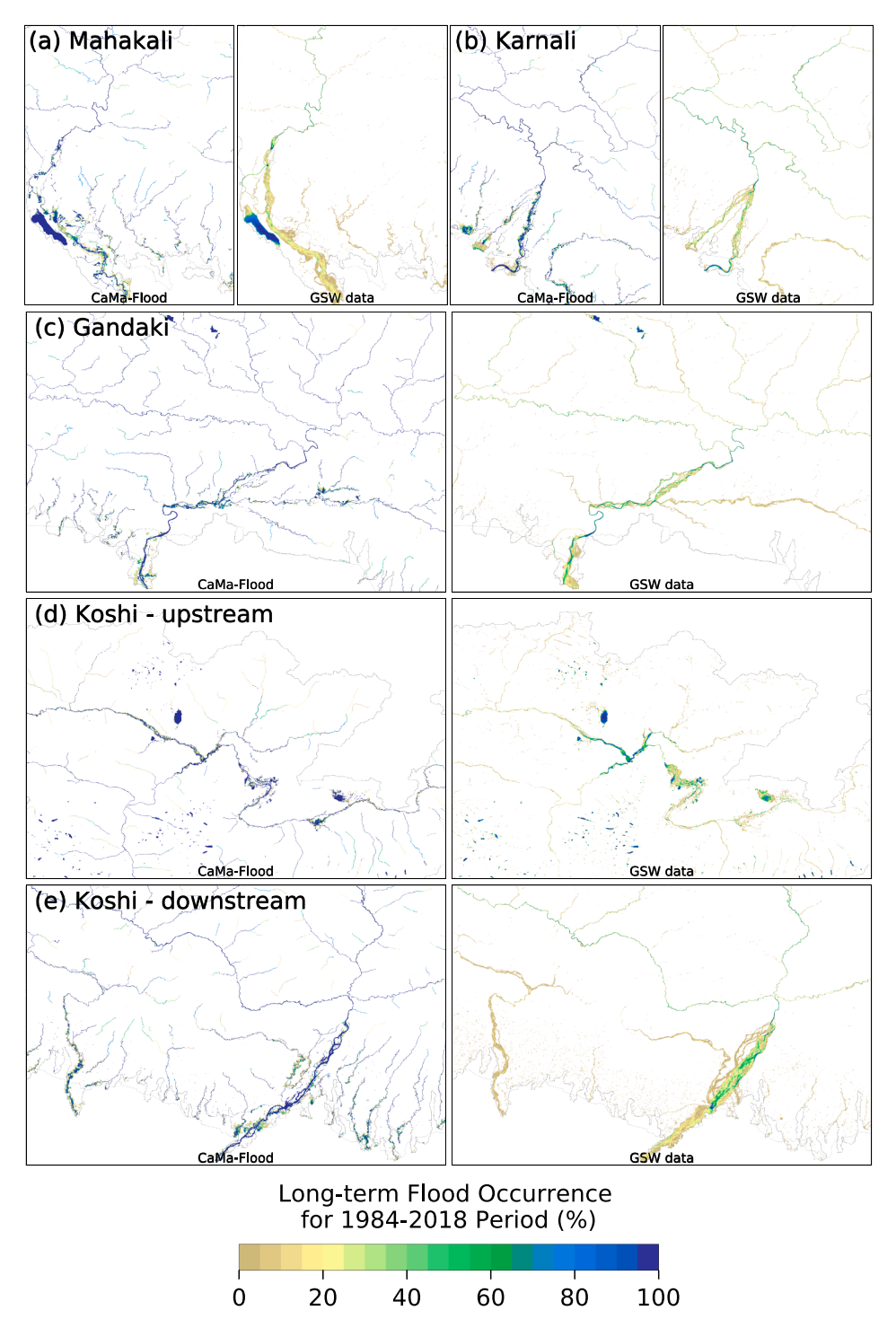


Fig. 6. Comparison of simulated flood occurrence (left; CaMa-Flood) with Landsat-based flood occurrence (right; GSW data). The selected regions are indicated in Fig. 5.

during 2002–2009 and a subsequent recovery of 0.92 (0.52) cm/year during 2010–2016 (Fig. 8). However, and as noted above, a continually declining trend (-1.67, -1.58, and -1.85 cm/year during 2002–2016, 2002–2009, and 2010–2016 periods, respectively) is found in the TWS from GRACE data that vertically integrate all TWS components. To examine the changes only in groundwater storage caused by natural variability and groundwater withdrawal, we use the results derived by using TWS from GRACE and simulated soil moisture and surface water storages (see Section 2.3). It is evident from Fig. 8 that the changes in the other TWS components than groundwater are relatively small and hence

the majority of the decline in TWS seen in GRACE comes from the decline in groundwater storage. The trends in groundwater storage change for the 2002–2016, 2002–2009, and 2010–2016 periods are -1.74, -1.46, and -2.18 cm/year, respectively, which closely align with the trends is GRACE-based TWS. Such consistent declines in the GRACE-based TWS and groundwater storage despite the recovery seen in the simulated TWS as well as groundwater storage suggest that human impacts have been intensifying in recent years. The contribution of human water use to TWS (and groundwater storage) change is estimated at -1.85 (-1.85) cm/year for 2002–2016 period and -1.37 (-1.36) and

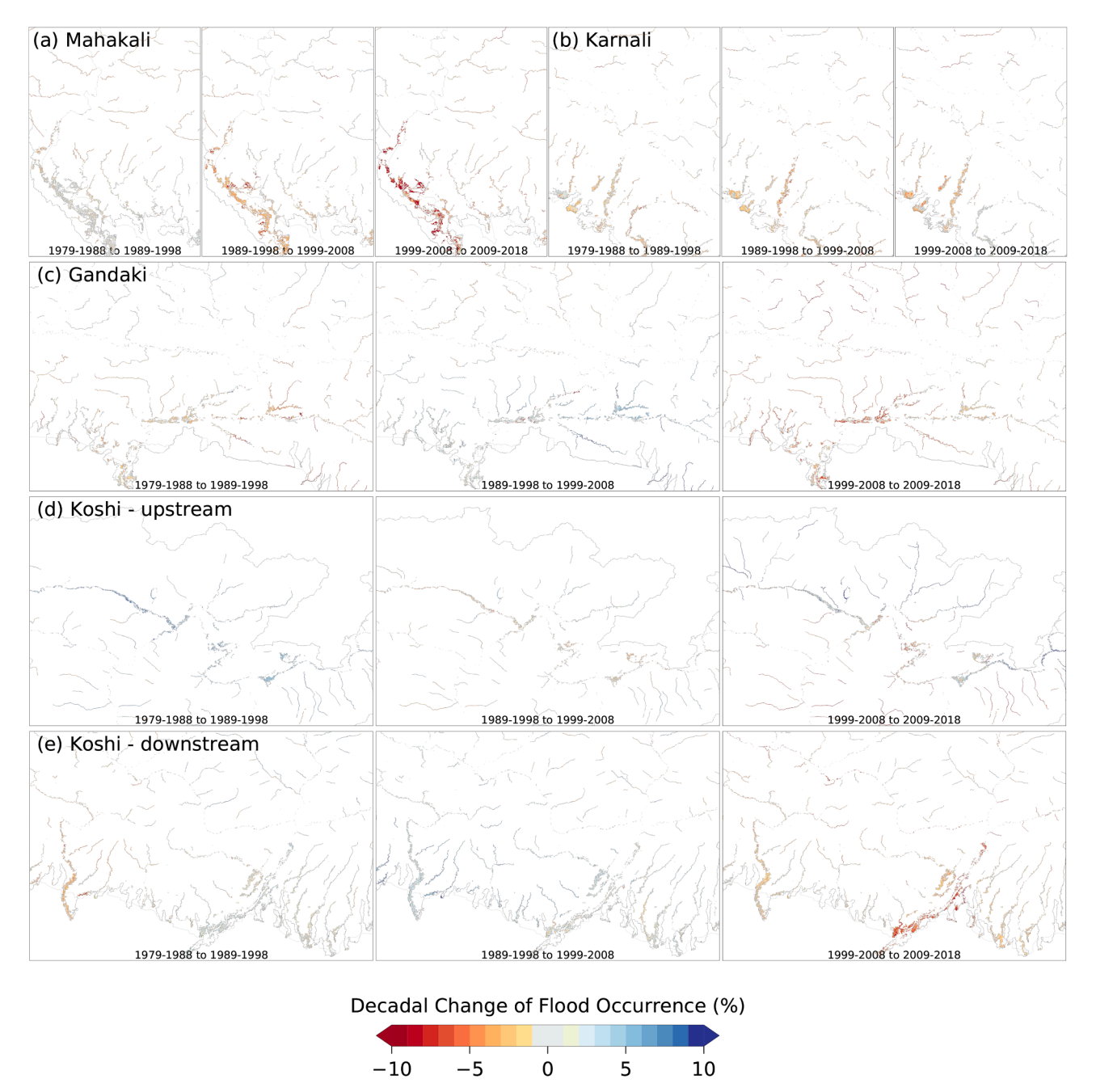


Fig. 7. Evolution of flood occurrence at the decadal interval. For each selected region, the decadal changes from 1979 to 1988 to 1989–1998 (left), from 1989 to 1998 to 1999–2008 (middle), and from 1999 to 2008 to 2009–2018 (right) periods are shown. The selected regions are indicated in Fig. 5.

-2.77 (-2.70) cm/year for 2002–2009 and 2010–2016 periods, respectively.

Even though the spatial scale for applying GRACE data, also referred to as the footprint, is $150,000\,\mathrm{km}^2$ or larger (Girotto et al., 2016; Li et al., 2012), the mascon products have been increasingly applied to even smaller areas in the range of $40,000-100,000\,\mathrm{km}^2$ (Scanlon et al., 2016). Our study domain ($\sim 196,000\,\mathrm{km}^2$) is larger than the footprint, but relatively small compared to sizes of major global basins (Scanlon et al., 2016). Hence, there can be uncertainties in the GRACE TWS and the groundwater storage change derived from it. However, the finding of declining trends of TWS and groundwater within Nepal and its surrounding regions is supported by other independent regional studies using various GRACE satellite products (e.g., Jing et al., 2019; Tiwari et al., 2009). Specifically, Tiwari et al. (2009) estimate the human-induced groundwater loss around Nepal to -1 to -4 cm/year for the

2002–2008 period, which aligns with the estimation of this study. In addition, well observation data of the Kathmandu Valley aquifer in central Nepal, which indicate a drawdown of groundwater levels by 1.38–7.5 m during 2000–2008 (Pandey et al., 2010; Shrestha et al., 2018), also support the finding of this study.

4. Summary and conclusion

This study presents the first results of the long-term (1979–2018) evolution of river-floodplain dynamics over all river basins of Nepal at a spatial resolution of $\sim 5~\rm km$ for river flow and $\sim 90~\rm m$ for flood extents. The simulated river discharge is validated nationally using the observations from DHM, Nepal. Using simulated results, historical changes in river discharge are then investigated using a quantile analysis method, which effectively describes the temporal evolution of river discharge, in

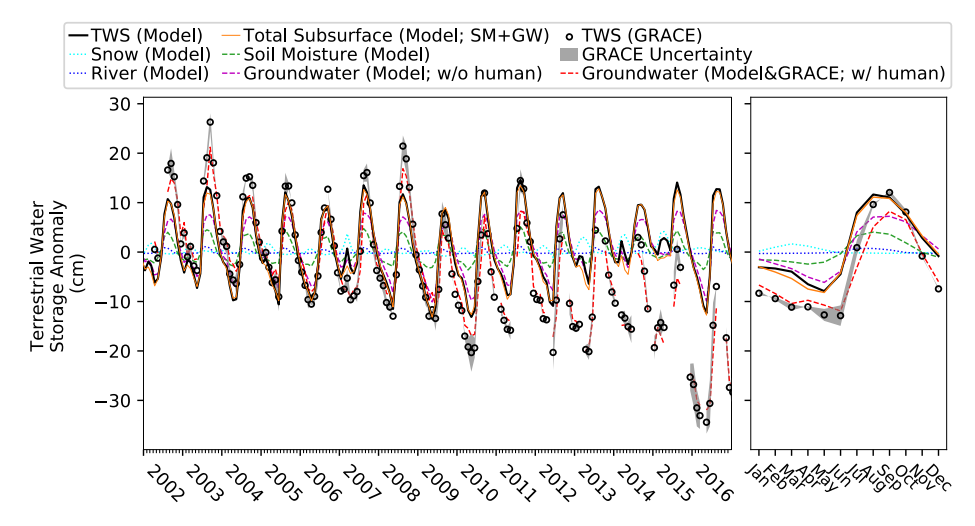


Fig. 8. TWS anomaly derived from GRACE data and HiGW-MAT & CaMa-Flood simulations averaged over the entire study domain (Fig. 1). The panel on the right shows the seasonal cycle. Grey shading indicates the uncertainty in GRACE data, expressed as the range between the two products.

terms of the long-term seasonality (QDAY), trend of seasonality change (QMOV), temporal evolution of seasonality (δ_{30d}), and change of flow duration curve (δ_{1vr}). Then, the spatio-temporal variations in river discharge are examined through mapping of decadal trends for low flow (Q_{10}) , median flow (Q_{50}) , and high flow (Q_{90}) . The long-term seasonality at the outlets of the major river basins is then analyzed using QDAY. The results of QMOV and δ_{30d} suggest that the high quantile flows during the wet season (i.e., JJAS) are persistently declining, especially during the latest two decades (1999–2018). Based on the analysis of δ_{1yr} and the decadal trends of flow duration curves, it is found that low, median, and high flows in the downstream regions have also decreased continually during the past two decades (1999-2018). Further, the annual flow duration curves are found to have evolved differently in different basins, and the evolution patterns of trends at the basin outlets generally coincide with those within the basins; however, some opposite patterns are also found within the basins in the northern part of Karnali, western part of Gandaki, and northern part of Koshi basins.

The comparison of high-resolution, simulated flood extent with satellite-based data suggest that the model reasonably reproduces the inundation extents in the major flooded areas, especially those in the southern parts of the country. Based on the evaluation of decadal changes in inundated areas over the major flooded regions, it is found that not only the changes in high quantile flows cause changes in inundation extent, but also the changes in low quantile flows modulate flood occurrence in riverine areas. Lastly, the changes in TWS during the 2002–2016 period is examined through combined use of model results and the GRACE data. Results suggest that the overall TWS dynamics is strongly modulated by the variations in subsurface water storage, and a growing influence of water management, especially a potential increase in groundwater use, has likely caused a continual decline in TWS and groundwater storage. The changes in GRACE TWS are found to be -1.67 cm/year during the 2002–2016 period and -1.58 and -1.85 cm/ year during the 2002-2009 and 2010-2016 periods, respectively. The changes in groundwater storage caused by both natural variability and ground water withdrawal, which is derived by combining model results and GRACE data, is estimated to be -1.74, -1.46, and -2.18 cm/year for the 2002-2016, 2002-2009, and 2010-2016 periods, respectively. There are certain limitations to this study, of which the most important one is the missing representation of water management processes in the models, especially groundwater use. The spatial resolution could also be further refined to better resolve hydrologic processes in the headwater catchments. Lastly, uncertainties might have been introduced to the GRACE TWS and the derived groundwater storage change because of the relatively small domain size. GRACE data when applied over small

domains may also suffer from leakage errors but those are expected to be small in the mascon products. Despite these limitations, this study presents a modeling framework consisting of a global land surface model and global floodplain hydrodynamics model with a promising capability to simulate the changing hydrology of the Himalayan region, providing a basis for improved understanding of the long-term hydrologic dynamics under climate change.

CRediT authorship contribution statement

Sanghoon Shin: Conceptualization, Methodology, Formal analysis, Investigation, Data curation, Writing - original draft, Visualization. Yadu Pokhrel: Conceptualization, Methodology, Investigation, Resources, Writing - original draft, Supervision, Project administration, Funding acquisition. Rocky Talchabhadel: Validation, Writing - review & editing. Jeeban Panthi: Vali, dation, Writing - review & editing.

Declaration of Competing Interest

The authors declare that they have no known competing financial interests or personal relationships that could have appeared to influence the work reported in this paper.

Acknowledgement

This study was partially supported by the National Science Foundation (Award#: 1752729) and the Asian Studies Center at MSU. Simulations were conducted using Cheyenne (doi:10.5065/D6RX99HX) provided by NCAR's Computational and Information Systems Laboratory, sponsored by the National Science Foundation. River discharge data is obtained from the Department of Hydrology and Meteorology, Nepal. Global Surface Water data are available from Google Earth Engine. CEEMDAN is performed using a Python package, PyEMD, developed by Dr. Dawid Laszuk.

References

Agarwal, A., Babel, M.S., Maskey, S., Shrestha, S., Kawasaki, A., Tripathi, N.K., 2016. Analysis of temperature projections in the Koshi River Basin, Nepal. Int. J. Climatol. 36 (1), 266–279. https://doi.org/10.1002/joc.4342.

Babel, M.S., Bhusal, S.P., Wahid, S.M., Agarwal, A., 2014. Climate change and water resources in the Bagmati River Basin. Nepal. Theor. Appl. Climatol. 115 (3-4), 639–654. https://doi.org/10.1007/s00704-013-0910-4.

Bajracharya, A.R., Bajracharya, S.R., Shrestha, A.B., Maharjan, S.B., 2018. Climate change impact assessment on the hydrological regime of the Kaligandaki Basin. Nepal. Sci. Total Environ. 625, 837–848. https://doi.org/10.1016/j. scitotenv.2017.12.332.

- Beven, K.J., Kirkby, M.J., 1979. A physically based, variable contributing area model of basin hydrology. Hydrol. Sci. Bull. 24, 43–69. https://doi.org/10.1080/ 02626667909491834
- Bharati, L., Gurung, P., Jayakody, P., Smakhtin, V., Bhattarai, U., 2014. The Projected Impact of Climate Change on Water Availability and Development in the Koshi Basin. Nepal. Mt. Res. Dev. 34 (2), 118–130. https://doi.org/10.1659/MRD-IOURNAL D.13.00065 1
- Bharati, L., Gurung, P., Maharjan, L., Bhattarai, U., 2016. Past and future variability in the hydrological regime of the Koshi Basin. Nepal. Hydrol. Sci. J. 61 (1), 79–93. https://doi.org/10.1080/02626667.2014.952639.
- Bhatta, B., Shrestha, S., Shrestha, P.K., Talchabhadel, R., 2019. Evaluation and application of a SWAT model to assess the climate change impact on the hydrology of the Himalayan River Basin. Catena 181, 104082. https://doi.org/10.1016/j. catena.2019.104082.
- Bonekamp, P.N.J., Collier, E., Immerzeel, W.W., 2018. The Impact of Spatial Resolution, Land Use, and Spinup Time on Resolving Spatial Precipitation Patterns in the Himalayas. J. Hydrometeorol. 19, 1565–1581. https://doi.org/10.1175/JHM-D-17-02121
- Bower, D., Hannah, D.M., McGregor, G.R., 2004. Techniques for assessing the climatic sensitivity of river flow regimes. Hydrol. Process. 18 (13), 2515–2543. https://doi. org/10.1002/hyp.1479.
- Burbano, M., Shin, S., Nguyen, K., Pokhrel, Y., 2020. Hydrologic changes, dam construction, and the shift in dietary protein in the Lower Mekong River Basin. J. Hydrol. 581, 124454. https://doi.org/10.1016/j.jhydrol.2019.124454.
- Chaudhari, S., Pokhrel, Y., Moran, E., Miguez-Macho, G., 2019. Multi-decadal hydrologic change and variability in the Amazon River basin: understanding terrestrial water storage variations and drought characteristics. Hydrol. Earth Syst. Sci. 23 (7), 2841–2862. https://doi.org/10.5194/hess-23-2841-2019.
- Chen, N.Sh., Hu, G.Sh., Deng, W., Khanal, N., Zhu, Y.H., Han, D., 2013. On the water hazards in the trans-boundary Kosi River basin. Nat. Hazards Earth Syst. Sci. 13, 795–808. https://doi.org/10.5194/nhess-13-795-2013.
- Chinnasamy, P., Bharati, L., Bhattarai, U., Khadka, A., Dahal, V., Wahid, S., 2015. Impact of planned water resource development on current and future water demand in the Koshi River basin. Nepal. Water Int. 40 (7), 1004–1020. https://doi.org/10.1080/ 02508060.2015.1099192.
- Colominas, M.A., Schlotthauer, G., Torres, M.E., 2014. Improved complete ensemble EMD: A suitable tool for biomedical signal processing. Biomed. Signal Process. Control 14, 19–29. https://doi.org/10.1016/j.bspc.2014.06.009.
- Dahal, N., Shrestha, U., Tuitui, A., Ojha, H., 2018. Temporal Changes in Precipitation and Temperature and their Implications on the Streamflow of Rosi River. Central Nepal. Climate 7, 3. https://doi.org/10.3390/cli7010003.
- Dahal, P., Shrestha, M.L., Panthi, J., Pradhananga, D., 2020. Modeling the future impacts of climate change on water availability in the Karnali River Basin of Nepal Himalaya. Environ. Res. 185, 109430. https://doi.org/10.1016/j.envres.2020.109430.
- Dhakal, S., Srivastava, L., Sharma, B., Palit, D., Mainali, B., Nepal, R., Purohit, P., Goswami, A., Malikyar, G.M., Wakhley, K.B., 2019. Meeting Future Energy Needs in the Hindu Kush Himalaya, in: The Hindu Kush Himalaya Assessment. Springer International Publishing, Cham, pp. 167–207. https://doi.org/10.1007/978-3-319-92288-1 6.
- Dhital, Y.P., Kayastha, R.B., 2013. Frequency analysis, causes and impacts of flooding in the Bagmati River Basin. Nepal. J. Flood Risk Manag. 6 (3), 253–260. https://doi. org/10.1111/jfr3.12013.
- Dimri, A.P., Kumar, D., Choudhary, A., Maharana, P., 2018a. Future changes over the Himalayas: Mean temperature. Glob. Planet. Change 162, 235–251. https://doi.org/ 10.1016/j.gloplacha.2018.01.014.
- Dimri, A.P., Kumar, D., Choudhary, A., Maharana, P., 2018b. Future changes over the Himalayas: Maximum and minimum temperature. Glob. Planet. Change 162, 212–234. https://doi.org/10.1016/j.gloplacha.2018.01.015.
- Felfelani, F., Wada, Y., Longuevergne, L., Pokhrel, Y.N., 2017. Natural and humaninduced terrestrial water storage change: A global analysis using hydrological models and GRACE. J. Hydrol. 553, 105–118. https://doi.org/10.1016/j. ihydrol.2017.07.048.
- Ferreira, V.G., Yong, B., Tourian, M.J., Ndehedehe, C.E., Shen, Z., Seitz, K., Dannouf, R., 2020. Characterization of the hydro-geological regime of Yangtze River basin using remotely-sensed and modeled products. Sci. Total Environ. 718, 137354. https://doi.org/10.1016/j.scitotenv.2020.137354.
- Friedman, R., Ansell, C., Diamond, S., Haimes, Y.Y., 1984. The Use of Models for Water Resources Management, Planning, and Policy. Water Resour. Res. 20 (7), 793–802. https://doi.org/10.1029/WR020i007p00793.
- Ghosh, S., Das, D., Kao, S.-C., Ganguly, A.R., 2012. Lack of uniform trends but increasing spatial variability in observed Indian rainfall extremes. Nat. Clim. Change 2 (2), 86–91. https://doi.org/10.1038/nclimate1327.
- Ghosh, S., Vittal, H., Sharma, T., Karmakar, S., Kasiviswanathan, K.S., Dhanesh, Y., Sudheer, K.P., Gunthe, S.S., Li, C., 2016. Indian Summer Monsoon Rainfall: Implications of Contrasting Trends in the Spatial Variability of Means and Extremes. PLOS ONE 11 (7), e0158670. https://doi.org/10.1371/journal.pone.0158670.
- Girotto, M., De Lannoy, G.J.M., Reichle, R.H., Rodell, M., 2016. Assimilation of gridded terrestrial water storage observations from GRACE into a land surface model. Water Resour. Res. 52 (5), 4164–4183. https://doi.org/10.1002/2015WR018417.
- Henriksen, H.J., Troldborg, L., Nyegaard, P., Sonnenborg, T.O., Refsgaard, J.C., Madsen, B., 2003. Methodology for construction, calibration and validation of a national hydrological model for Denmark. J. Hydrol. 280 (1-4), 52–71. https://doi. org/10.1016/S0022-1694(03)00186-0.
- Immerzeel, W.W., Petersen, L., Ragettli, S., Pellicciotti, F., 2014. The importance of observed gradients of air temperature and precipitation for modeling runoff from a

- glacierized watershed in the Nepalese Himalayas. Water Resour. Res. 50 (3), 2212–2226. https://doi.org/10.1002/2013WR014506.
- Immerzeel, W.W., van Beek, L.P.H., Bierkens, M.F.P., 2010. Climate Change Will Affect the Asian Water Towers. Science 328 (5984), 1382–1385. https://doi.org/10.1126/ science 1183188
- Immerzeel, W.W., Wanders, N., Lutz, A.F., Shea, J.M., Bierkens, M.F.P., 2015. Reconciling high-altitude precipitation in the upper Indus basin with glacier mass balances and runoff. Hydrol. Earth Syst. Sci. 19, 4673–4687. https://doi.org/ 10.5194/hess-19-4673-2015.
- Jeelani, G., Feddema, J.J., van der Veen, C.J., Stearns, L., 2012. Role of snow and glacier melt in controlling river hydrology in Liddar watershed (western Himalaya) under current and future climate. Water Resour. Res. 48 (12) https://doi.org/10.1029/ 2011WR011590
- Jing, W., Zhang, P., Zhao, X., 2019. A comparison of different GRACE solutions in terrestrial water storage trend estimation over Tibetan Plateau. Sci. Rep. 9, 1765. https://doi.org/10.1038/s41598-018-38337-1.
- Karki, R., Talchabhadel, R., Aalto, J., Baidya, S.K., 2016. New climatic classification of Nepal. Theor. Appl. Climatol. 125 (3-4), 799–808. https://doi.org/10.1007/s00704-015-1549-0
- Karki, R., ul Hasson, S., Gerlitz, L., Talchabhadel, R., Schickhoff, U., Scholten, T., Böhner, J., 2020. Rising mean and extreme near-surface air temperature across Nepal. Int. J. Climatol. 40 (4), 2445–2463. https://doi.org/10.1002/joc.6344.
- Koirala, S., Yeh, P.-F., Hirabayashi, Y., Kanae, S., Oki, T., 2014. Global-scale land surface hydrologic modeling with the representation of water table dynamics. J. Geophys. Res. 119 (1), 75–89. https://doi.org/10.1002/2013JD020398.
- Li, B., Rodell, M., Zaitchik, B.F., Reichle, R.H., Koster, R.D., van Dam, T.M., 2012. Assimilation of GRACE terrestrial water storage into a land surface model: Evaluation and potential value for drought monitoring in western and central Europe. J. Hydrol. 446–447, 103–115. https://doi.org/10.1016/j. ibvdrol.2012.04.035.
- McMillan, H.K., Booker, D.J., Cattoën, C., 2016. Validation of a national hydrological model. J. Hydrol. 541, 800–815. https://doi.org/10.1016/j.jhydrol.2016.07.043.
- Mishra, Y., Nakamura, T., Babel, M.S., Ninsawat, S., Ochi, S., 2018. Impact of climate change on water resources of the Bheri River Basin. Nepal. Water Switz. 10, 1–21. https://doi.org/10.3390/w10020220.
- Mitra, C., Shepherd, J.M., Jordan, T., 2012. On the relationship between the premonsoonal rainfall climatology and urban land cover dynamics in Kolkata city. India. Int. J. Climatol. 32 (9), 1443–1454. https://doi.org/10.1002/joc.2366.
- Nazemi, A., Wheater, H.S., 2015. On inclusion of water resource management in Earth system models—part 1: problem definition and representation of water demand. Hydrol Earth Syst Sci 19 (1), 33–61. https://doi.org/10.5194/hess-19-33-2015.
- Palazzoli, I., Maskey, S., Uhlenbrook, S., Nana, E., Bocchiola, D., 2015. Impact of prospective climate change on water resources and crop yields in the Indrawati basin. Nepal. Agric. Syst. 133, 143–157. https://doi.org/10.1016/j. agsv.2014.10.016.
- Pandey, V.P., Babel, M.S., Shrestha, S., Kazama, F., 2011. A framework to assess adaptive capacity of the water resources system in Nepalese river basins. Ecol. Indic. 11 (2), 480–488. https://doi.org/10.1016/j.ecolind.2010.07.003.
- Pandey, V.P., Chapagain, S.K., Kazama, F., 2010. Evaluation of groundwater environment of Kathmandu Valley. Environ. Earth Sci. 60 (6), 1329–1342. https://doi.org/10.1007/s12665-009-0263-6.
- Pandey, V.P., Dhaubanjar, S., Bharati, L., Thapa, B.R., 2019. Hydrological response of Chamelia watershed in Mahakali Basin to climate change. Sci. Total Environ. 650, 365–383. https://doi.org/10.1016/j.scitotenv.2018.09.053.
- Prasad Pandey, V., Kazama, F., 2014. From an open-access to a state-controlled resource: the case of groundwater in the Kathmandu Valley. Nepal. Water Int. 39 (1), 97–112. https://doi.org/10.1080/02508060.2014.863687.
- Panthi, J., Dahal, P., Shrestha, M.L., Aryal, S., Krakauer, N.Y., Pradhanang, S.M., Lakhankar, T., Jha, A.K., Sharma, M., Karki, R., 2015. Spatial and temporal variability of rainfall in the Gandaki River Basin of Nepal Himalaya. Climate 3, 210–226. https://doi.org/10.3390/cli3010210.
- Paudel, B., Gao, J., Zhang, Y., Wu, X., Li, S., Yan, J., 2016. Changes in Cropland Status and Their Driving Factors in the Koshi River Basin of the Central Himalayas. Nepal. Sustainability 8, 933. https://doi.org/10.3390/su8090933.
- Pekel, J.-F., Cottam, A., Gorelick, N., Belward, A.S., 2016. High-resolution mapping of global surface water and its long-term changes. Nature 540 (7633), 418–422. https://doi.org/10.1038/nature20584.
- Pokhrel, Y., Hanasaki, N., Koirala, S., Cho, J., Yeh, P.-J.-F., Kim, H., Kanae, S., Oki, T., 2012a. Incorporating Anthropogenic Water Regulation Modules into a Land Surface Model. J. Hydrometeorol. 13, 255–269. https://doi.org/10.1175/JHM-D-11-013.1.
- Pokhrel, Y., Hanasaki, N., Yeh, P.J.F., Yamada, T.J., Kanae, S., Oki, T., 2012b. Model estimates of sea-level change due to anthropogenic impacts on terrestrial water storage. Nat. Geosci. 5, 389–392. https://doi.org/10.1038/ngeo1476.
- Pokhrel, Y., Shin, S., Lin, Z., Yamazaki, D., Qi, J., 2018. Potential Disruption of Flood Dynamics in the Lower Mekong River Basin Due to Upstream Flow Regulation. Sci. Rep. 8, 17767. https://doi.org/10.1038/s41598-018-35823-4.
- Pokhrel, Y.N., Felfelani, F., Shin, S., Yamada, T.J., Satoh, Y., 2017. Modeling large-scale human alteration of land surface hydrology and climate. Geosci. Lett. 4, 10. https:// doi.org/10.1186/s40562-017-0076-5.
- Pokhrel, Y.N., Hanasaki, N., Wada, Y., Kim, H., 2016. Recent progresses in incorporating human land-water management into global land surface models toward their integration into Earth system models. Wiley Interdiscip. Rev. Water. https://doi.org/ 10.1002/wat2.1150.
- Pokhrel, Y.N., Koirala, S., Yeh, P.-F., Hanasaki, N., Longuevergne, L., Kanae, S., Oki, T., 2015. Incorporation of groundwater pumping in a global Land Surface Model with

- the representation of human impacts. Water Resour. Res. 51 (1), 78–96. https://doi.org/10.1002/2014WR015602.
- Poudyal, R., Loskot, P., Nepal, R., Parajuli, R., Khadka, S.K., 2019. Mitigating the current energy crisis in Nepal with renewable energy sources. Renew. Sustain. Energy Rev. 116, 109388. https://doi.org/10.1016/j.rser.2019.109388.
- Rajbhandari, R., Shrestha, A.B., Nepal, S., Wahid, S., Ren, G.-Y., 2017. Extreme climate projections over the transboundary Koshi River Basin using a high resolution regional climate model. Adv. Clim. Change Res. 8 (3), 199–211. https://doi.org/10.1016/j.accre.2017.08.006.
- Richards, L.A., 1931. Capillary conduction of liquids through porous mediums. J. Appl. Phys. 1 (5), 318–333. https://doi.org/10.1063/1.1745010.
- Rodell, M., Velicogna, I., Famiglietti, J.S., 2009. Satellite-based estimates of groundwater depletion in India. Nature 460 (7258), 999–1002. https://doi.org/10.1038/ nature08238.
- Rottler, E., Francke, T., Bürger, G., Bronstert, A., 2019. Long-term changes in Central European river discharge 1869–2016: impact of changing snow covers, reservoir constructions and an intensified hydrological cycle. Hydrol. Earth Syst. Sci. Discuss. 24, 1–32. https://doi.org/10.5194/hess-2019-487.
- Roy, J., Moors, E., Murthy, M.S.R., Prabhakar, S.V.R.K., Khattak, B.N., Shi, P., Huggel, C., Chitale, V., 2019. In: The Hindu Kush Himalaya Assessment: Mountains, Climate Change, Sustainability and People. Springer International Publishing, Cham, pp. 99–125. https://doi.org/10.1007/978-3-319-92288-1_4.
- Save, H., Bettadpur, S., Tapley, B.D., 2016. High-resolution CSR GRACE RL05 mascons.
 J. Geophys. Res. Solid Earth 121 (10), 7547–7569. https://doi.org/10.1002/ 2016.IB013007
- Scanlon, B.R., Zhang, Z., Save, H., Wiese, D.N., Landerer, F.W., Long, D.i., Longuevergne, L., Chen, J., 2016. Global evaluation of new GRACE mascon products for hydrologic applications. Water Resour. Res. 52 (12), 9412–9429. https://doi. org/10.1002/2016WR019494.
- Sellers, P.J., 1997. Modeling the Exchanges of Energy, Water, and Carbon Between Continents and the Atmosphere. Science 275, 502–509. https://doi.org/10.1126/ psience/275-5206-523
- Sen, P.K., 1968. Estimates of the Regression Coefficient Based on Kendall's Tau. J. Am. Stat. Assoc. 63 (324), 1379–1389. https://doi.org/10.1080/ 01621459.1968.10480934.
- Sharma, R.H., Shakya, N.M., 2006. Hydrological changes and its impact on water resources of Bagmati watershed. Nepal. J. Hydrol. 327 (3-4), 315–322. https://doi. org/10.1016/j.jhydrol.2005.11.051.
- Shin, S., Pokhrel, Y., Huang, X., Torbick, N., Qi, J., Pattanakiat, S., Ngo-Duc, T., Tuan, N. D., 2020. High Resolution Modeling of River-floodplain-reservoir Inundation Dynamics in the Mekong River Basin. Water Resour. Res. 56 (5), e2019WR026449 https://doi.org/10.1029/2019WR026449.
- Shrestha, M.L., 2000. Interannual variation of summer monsoon rainfall over Nepal and its relation to Southern Oscillation Index. Meteorol. Atmospheric Phys. 75 (1-2), 21–28. https://doi.org/10.1007/s007030070012.
- Shrestha, S., Gyawali, B., Bhattarai, U., 2013. Impacts of climate change on irrigation water requirements for rice-wheat cultivation in Bagmati River Basin. Nepal. J. Water Clim. Change 4, 422–439. https://doi.org/10.2166/wcc.2013.050.
- Water Clim. Change 4, 422–439. https://doi.org/10.2166/wcc.2013.050.

 Shrestha, S., Khatiwada, M., Babel, M.S., Parajuli, K., 2014. Impact of Climate Change on River Flow and Hydropower Production in Kulekhani Hydropower Project of Nepal. Environ. Process. 1 (3), 231–250. https://doi.org/10.1007/s40710-014-0020-z.
- Shrestha, S., Neupane, S., Mohanasundaram, S., Pandey, V.P., 2020. Mapping groundwater resiliency under climate change scenarios: A case study of Kathmandu Valley. Nepal. Environ. Res. 183, 109149. https://doi.org/10.1016/j. envres 2020.109149
- Shrestha, S., Semkuyu, D.J., Pandey, V.P., 2016a. Assessment of groundwater vulnerability and risk to pollution in Kathmandu Valley. Nepal. Sci. Total Environ. 556, 23–35. https://doi.org/10.1016/j.scitoteny.2016.03.021.
- Shrestha, S., Shrestha, M., Babel, M.S., 2016b. Modelling the potential impacts of climate change on hydrology and water resources in the Indrawati River Basin. Nepal. Environ. Earth Sci. 75, 1–13. https://doi.org/10.1007/s12665-015-5150-8.
- Shrestha, S.R., Tripathi, G.N., Laudari, D., 2018. Groundwater Resources of Nepal: An Overview. In: Mukherjee, A. (Ed.), Groundwater of South Asia. Springer Singapore, Singapore, pp. 169–193. https://doi.org/10.1007/978-981-10-3889-1_11.
- Shrestha, U.B., Gautam, S., Bawa, K.S., Bohrer, G., 2012. Widespread Climate Change in the Himalayas and Associated Changes in Local Ecosystems. PLoS ONE 7 (5), e36741. https://doi.org/10.1371/journal.pone.0036741.

- Singh, S.P., Sharma, S., Dhyani, P.P., 2019. Himalayan arc and treeline: distribution, climate change responses and ecosystem properties. Biodivers. Conserv. 28 (8-9), 1997–2016. https://doi.org/10.1007/s10531-019-01777-w.
- Stieglitz, M., Rind, D., Famiglietti, J., Rosenzweig, C., 1997. An efficient approach to modeling the topographic control of surface hydrology for regional and global climate modeling. J. Clim. 10, 118–137. https://doi.org/10.1175/1520-0442(1997) 010-0118:AEATMT-2.0.CO:2.
- Takata, K., Emori, S., Watanabe, T., 2003. Development of the minimal advanced treatments of surface interaction and runoff. Glob. Planet. Change 38 (1-2), 209–222. https://doi.org/10.1016/S0921-8181(03)00030-4.
- Tewari, V.P., Verma, R.K., von Gadow, K., 2017. Climate change effects in the Western Himalayan ecosystems of India: evidence and strategies. For. Ecosyst. 4, 13. https://doi.org/10.1186/s40663-017-0100-4.
- Tiwari, V.M., Wahr, J., Swenson, S., 2009. Dwindling groundwater resources in northern India, from satellite gravity observations. Geophys. Res. Lett. 36, L18401. https://doi.org/10.1029/2009GL039401.
- Torres, M.E., Colominas, M.A., Schlotthauer, G., Flandrin, P., 2011. A complete ensemble empirical mode decomposition with adaptive noise, in: ICASSP, IEEE International Conference on Acoustics, Speech and Signal Processing - Proceedings. IEEE, pp. 4144–4147. https://doi.org/10.1109/ICASSP.2011.5947265.
- Viviroli, D., Dürr, H.H., Messerli, B., Meybeck, M., Weingartner, R., 2007. Mountains of the world, water towers for humanity: Typology, mapping, and global significance. Water Resour. Res. 43 (7) https://doi.org/10.1029/2006WR005653.
- Wada, Y., Bierkens, M.F.P., de Roo, A., Dirmeyer, P.A., Famiglietti, J.S., Hanasaki, N., Konar, M., Liu, J., Müller Schmied, H., Oki, T., Pokhrel, Y., Sivapalan, M., Troy, T.J., van Dijk, A.I.J.M., van Emmerik, T., Van Huijgevoort, M.H.J., Van Lanen, H.A.J., Vörösmarty, C.J., Wanders, N., Wheater, H., 2017. Human-water interface in hydrological modeling: Current status and future directions. Hydrol. Earth Syst. Sci. 21, 4169–4193. https://doi.org/10.5194/hess-21-4169-2017.
- Watkins, M.M., Wiese, D.N., Yuan, D.-N., Boening, C., Landerer, F.W., 2015. Improved methods for observing Earth's time variable mass distribution with GRACE using spherical cap mascons. J. Geophys. Res. Solid Earth 120 (4), 2648–2671. https://doi. org/10.1002/2014JB011547.
- Weedon, G.P., Balsamo, G., Bellouin, N., Gomes, S., Best, M.J., Viterbo, P., 2018. The WFDEI Meteorological Forcing Data. Research Data Archive at the National Center for Atmospheric Research, Computational and Information Systems Laboratory, Boulder CO. https://doi.org/10.5065/486N-8109.
- Yamazaki, D., de Almeida, G.A.M., Bates, P.D., 2013. Improving computational efficiency in global river models by implementing the local inertial flow equation and a vector-based river network map. Water Resour. Res. 49 (11), 7221–7235. https://doi.org/10.1002/wrcr.20552.
- Yamazaki, D., Ikeshima, D., Sosa, J., Bates, P.D., Allen, G.H., Pavelsky, T.M., 2019. MERIT Hydro: A high-resolution global hydrography map based on latest topography datasets. Water Resour. Res. 55 (6), 5053–5073. https://doi.org/ 10.1029/2019WR024873.
- Yamazaki, D., Ikeshima, D., Tawatari, R., Yamaguchi, T., O'Loughlin, F., Neal, J.C., Sampson, C.C., Kanae, S., Bates, P.D., 2017. A high-accuracy map of global terrain elevations. Geophys. Res. Lett. 44 (11), 5844–5853. https://doi.org/10.1002/ 2017GI072874.
- Yamazaki, D., Kanae, S., Kim, H., Oki, T., 2011. A physically based description of floodplain inundation dynamics in a global river routing model. Water Resour. Res. 47 (4) https://doi.org/10.1029/2010WR009726.
- Yamazaki, D., Lee, H., Alsdorf, D.E., Dutra, E., Kim, H., Kanae, S., Oki, T., 2012. Analysis of the water level dynamics simulated by a global river model: A case study in the Amazon River. Water Resour. Res. 48 (9) https://doi.org/10.1029/2012WR011869. Yamazaki, D., Sato, T., Kanae, S., Hirabayashi, Y., Bates, P.D., 2014. Regional flood
- Yamazaki, D., Sato, T., Kanae, S., Hirabayashi, Y., Bates, P.D., 2014. Regional flood dynamics in a bifurcating mega delta simulated in a global river model. Geophys. Res. Lett. 41 (9), 3127–3135. https://doi.org/10.1002/2014GL059744.
- Yeh, P.J.F., Eltahir, E.A.B., 2005. Representation of water table dynamics in a land surface scheme. Part I: Model development. J. Clim. 18, 1861–1880. https://doi.org/ 10.1175/JCLI3330.1.
- Zhao, F., Veldkamp, T.I.E., Frieler, K., Schewe, J., Ostberg, S., Willner, S., Schauberger, B., Gosling, S.N., Schmied, H.M., Portmann, F.T., Leng, G., Huang, M., Liu, X., Tang, Q., Hanasaki, N., Biemans, H., Gerten, D., Satoh, Y., Pokhrel, Y., Stacke, T., Ciais, P., Chang, J., Ducharne, A., Guimberteau, M., Wada, Y., Kim, H., Yamazaki, D., 2017. The critical role of the routing scheme in simulating peak river discharge in global hydrological models. Environ. Res. Lett. 12 (7), 075003. https://doi.org/10.1088/1748-9326/aa7250.